Symkom 2014 **Open Access**

Artur Dróżdż and Witold Elsner*

Analysis of hot-wire measurements accuracy in turbulent boundary layer

DOI 10.1515/eng-2015-0033

Received January 23, 2015; accepted May 13, 2015

Abstract: This paper discusses the issue of measuring velocity fluctuations of turbulent boundary layer using hot-wire probes. The study highlights the problem of spatial resolution, which is essential when measuring small-scales in wall-bounded flows. Additionally, attention was paid to the inconsistency in streamwise fluctuation measurements using single- and X-wire probes. To clarify this problem, the energy spectra using wavelet transformation were calculated. The analysis was performed for turbulent boundary layer flow, which was characterized by Reynolds number based on the friction velocity equal $Re_\tau \approx 1000$.

Keywords: turbulent boundary layer; hot-wire; spatial resolution; energy spectra

1 Introduction

Hot-wire anemometry (HWA) is still one of the most common techniques used for turbulent boundary layer investigation. Insufficient spatial resolution of hot-wire probes causes problems in the measurement of small-scale turbulence, especially in high Reynolds number flows. The most well-known study discussing this problem is that by Ligrani and Bradshaw [1], which describes an extensive study of the effects of wire length on the data obtained from single hot-wire experiments. According to common opinion, a hot-wire anemometry using a single-wire probe is sufficient to resolve the streamwise velocity component u_x [2], however an influence of the wall-normal u_y component on a single-wire probe readings has not been thoroughly discussed. One should be aware that a single-wire probe measures not the u_x component, but also the resultant velocity, composed of both u_x and u_y . The subscripts x, y and z correspods relatively to: streamwise, wall-normal and spanwise flow directions.

Most researchers who perform measurements in turbulent boundary layer believe that the influence of the u_y component is insignificant and can be ignored. The comparison of u_x fluctuation distributions obtained with DNS (Direct Numerical Simulation) and from a single-wire probe have revealed self-similarity in shape [3, 4]. Some differences observed in levels of fluctuations were attributed mainly to the uncertainty error, not to the u_y component. It seems, however, that that such a belief of a negligible small influence of u_y on a single-wire readings is not justified. Despite the predominant motion of the streamwise direction, the vortical structure that is present in a turbulent boundary layer has to act on the probe wire, inducing an u_y velocity component. This was confirmed by the DNS study of Lenaers *et al.* [5] who observed the high value of wall-normal velocity fluctuations, which occasionally occur in the near-wall region and have larger magnitude than their local standard deviation.

Investigations performed by Dróżdż and Elsner [6], based on the measurements of zero pressure gradient (ZPG) turbulent boundary layer with single and X-wire probes, aimed to clarify the effect of the wall-normal component on the readings of single-wire probe in the vicinity to the inner peak of velocity fluctuations. They showed that the difference between streamwise fluctuating component measured with single and X-wire probes results not only from spatial resolution, but also from influence of wall normal fluctuating component, which is usually not considered. Such an effect results from the near-wall vortical structures inducing strong u_y component in the case where the mean velocity U has the lowest value [6]. In the present paper we present an extension of those studies, considering additional measurements from turbulent boundary layer subjected to an adverse pressure gradient (APG) that induces a second peak of velocity fluctuations in the outer region. It is believed that the second peak is a result of large-scale motions and it can confirm the more pronounced contribution of outer region to the downstream development of turbulent boundary layer [7].

Artur Dróżdż: Czestochowa Univ. of Tech., Armii Krajowej 21, 42-201, Czestochowa, Poland

***Corresponding Author: Witold Elsner:** Czestochowa Univ. of Tech., Armii Krajowej 21, 42-201, Czestochowa, Poland, E-mail: welsner@imc.pcz.czest.pl

2 Methodology and instrumentation

The experiment was performed in an open-circuit wind tunnel, where the turbulent boundary layer was developed along a flat plate, which was 2807 mm long by 250 mm wide. The upper wall of the rear part of the test section, presented in Figure 1, was shaped according to the assumed distribution of pressure gradient corresponding to the conditions encountered in the axial compressor blading. The intake channel height was 155 mm, while the boundary layer thickness δ was up to 25 mm. The facility had two pairs of suction gaps, located in the channel upstream of the test section, aimed at controlling the two-dimensionality of the flow. To avoid separation, the leading edge of the flat plate had an elliptical shape. The tripping of the boundary layer, after the leading edge of the plate, was used to obtain fully developed turbulence, and it allowed to obtain value of Reynolds number, equal to $Re_\tau = \frac{u_\tau \delta}{\upsilon} \approx 1000$, where υ is kinematic viscosity, based on the frictional velocity $u_\tau = \sqrt{\mu \frac{dU}{dy}}$. The frictional velocity was obtained based on the Fringe Skin Friction (FSF) method [8] and was verified with a Clauser plot.

The facility was equipped with the computer-controlled 2D traversing system (in streamwise and wall-normal directions). The traverse carriage was driven over a maximum displacement of 180 mm by a servo-motor. Uncertainty of the drive step was 0.001 mm, with the smallest step equal to 0.01 mm. The wall closest position of the hot-wire probe was determined using the mirrored image. Further details of the test section is given in Dróżdż *et al.* (2015) [9].

The mean velocity in core flow was $U_\infty \approx 15$ m/s and turbulence intensity was $Tu = 0.4\%$. The ambient conditions were carefully controlled during the measurements. The variation of ambient temperature at the end of the test section did not exceed 0.2°. When the measured temperature was different from temperature during calibration, the temperature correction of CTA voltage was used [10]. At the same time the free-stream velocity was monitored by the means of a Prandtl tube. The variability of free-stream velocity was found to be around 0.2% of the mean value. The convergence of the flow statistics up to 4th order was checked during preliminary tests. The convergence was achieved after approximately 3.5 s while the acquisition time was equal to 10 s.

For the purpose of the work in this paper, data from two traverses taken at zero (Sg= 0.185, blue thick line) and at the adverse pressure gradient region (Sg=0.738, red thick line) were considered. Sg corresponds to dimensionless distance from inlet plane (Sg=0) of the measuring section, which is located 1740 mm downstream from the leading edge. Velocity profiles were measured with single hot-wire anemometry probes of diameter $d = 3\mu$m and length $l = 0.4$ mm (Dantec Dynamics 55P31) and $d = 5\mu$m and length $l = 1.25$ mm (Dantec Dynamics 55P01). Those measurements were supplemented with X-wire probe of wire diameter $d = 5\mu$m and length $l = 1.5$ mm (Dantec Dynamics 55P61). The probes were combined with the DISA 55M hot-wire bridge connected to a 14 bit PC card. The acquisition was maintained at frequency $f = 50$ kHz with 10 seconds sampling records. For the assumed sampling frequency, the non-dimensional inner scale representation was $f^+ = f_\nu/u_\tau^2 \approx 1$. It was consistent with the assumption of Hutchins *et al.* (2009) [2], noting that for the proper anemometer/probe response, cutoff must be in the range of $f^+ > 1/3 (t^+ < 3)$, where $t^+ = 1/f^+$ is the non-dimensional sampling period.

3 Discussion of the results

Spatial averaging due to the large length of the single-wire is known to reduce the near-wall peak of turbulence intensity [1], but also it could falsify higher order moments, like the skewness and flatness factors [11]. It could also reduce the frequency of detected burst events as documented by Johansson and Alfredsson [12]. Ligrani and Bradshaw [1] found two key recommendations for accurate measurements, and both have become standards for hot-wire design: i.e. $l^+ \leq 20$ and $l/d > 200$, where l is length of a wire (in the viscous units $l^+ = lu_\tau/\nu$, while d is wire diameter. To satisfy these conditions in our research, the miniature probe, with length of the wire $l = 0.4$ mm and diameter of $d = 3\mu$m, also characterized by $l/d = 133$, was used. The l/d value did not fulfill the recommendation of Ligrani and Bradshaw [1], however Dróżdż and Elsner [6] demonstrated, by comparing the fluctuation distributions measured by miniature wire probe ($l = 0.4$ mm) with the standard wire probe of $l = 1.25$ mm, that the use of the first probe allows for increasing of the frequency of detected burst events. As a result, the magnitude of the near-wall peak increased by 10% and reached a value of $\overline{uu}^+ = \overline{uu}/u_\tau^2 \approx 8$, which is typical for the analyzed Reynolds number. Another inconsistency in streamwise fluctuation distributions, discussed in the paper, results from using different types of probe. To analyze the problem, the velocity fluctuations from single and Xwire probes were measured in two different traverses of the test section. For the

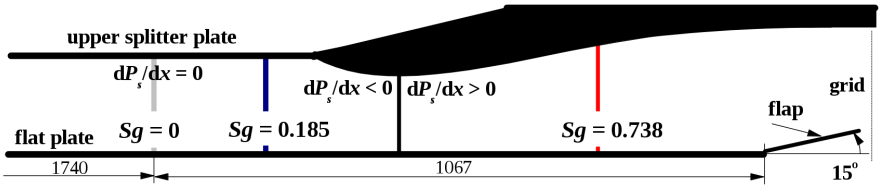

Figure 1: Shape of test section with locations of measured traverses.

first one taken at zero pressure gradient (Sg = 0.185) friction velocity was equal to about $u_\tau \approx 0.63$, which allowed to obtain $l^+ \approx 16$ for the single-wire probe and $l^+ \approx 50$ for the X-wire probe. For the second one taken at the adverse pressure gradient (Sg = 0.738) friction velocity was equal to about $u_\tau \approx 0.37$, which allowed to obtain $l^+ \approx 25$ for the single-wire probe and $l^+ \approx 25$ for X-wire probe.

It may be noticed from Figure 2a that for Sg = 0.185 the distribution of $\overline{uu}^+$ obtained by means of single-wire probe reveals a single peak located at $y^+ = yu_\tau/\nu \approx 15$, which is typical for turbulent boundary layers at zero pressure gradient. This peak location is not, however, reached for X-wire probe due to a large probe size, which is not able to penetrate the boundary layer as close as the single-wire probe. It should also be noticed that the streamwise $\overline{uu}^+$ and $\overline{uu}^+_x$ distributions for single and X-wire probes, respectively, are clearly different. In order to emphasize this difference, $\overline{uu}^+$ measured by single-wire is introduced without subscript x. On the other hand, computations of the resultant velocity fluctuations in xy plane i.e. $\overline{uu}^+_{xy} = \left(\overline{uu}^2_x + \overline{uu}^2_y\right)^{\frac{1}{2}}/u^2_\tau$ uing the values obtained with X-wire probe show nearly identical shape to the streamwise $\overline{uu}^+$ obtained with single-wire probe. The slightly higher values of $\overline{uu}^+_{xy}$ obtained from X-wire probe could be due to influence of the spanwise $\overline{uu}^+_z$ component, which somewhat increases the readings of X-wire probe, but does not do so in case of a single-wire, where the spanwise influence is minor due to the same direction as the direction of a wire axis. It should be kept in mind that this influence could also be partly attenuated by the larger measuring volume of X-wire probe.

For Sg = 0.783, due to the much thicker boundary layer, X-wire measurements reach single-wire values at $y^+ \approx 10$. In this case (Figure 2b), at $y^+ \approx 250$ both measurements exhibit the so called outer peak, which has been observed by many authors [13–15] for turbulent boundary layer subjected to adverse pressure gradient. The inner peak at this location is almost invisible. It can be noticed that the streamwise $\overline{uu}^+$ and $\overline{uu}^+_{xy}$ distributions almost overlap, which is not the case for Sg = 0.185, because of the same l^+ for both probes, therefore spatial averaging is not occurring. The $\overline{uu}^+_{xy}$ obtained from X-wire probe is substantially larger than $\overline{uu}^+$ from single-wire; however the difference between $\overline{uu}^+_x$ and $\overline{uu}^+_{xy}$ is of the same order as for ZPG traverse, where spatial averaging effect of the X-wire probe counteracts against the spanwise $\overline{uu}^+_z$ component. For APG traverse the results measured by both probes are free from spatial averaging, and $\overline{uu}^+_{xy}$ obtained by X-wire probe is affected by $\overline{uu}^+_z$ component. It could be concluded that the readings of single-wire probe are highly influenced by $\overline{uu}^+_y$ fluctuations, however it is not as strong in case of APG, because the $\overline{uu}^+_y$ to $\overline{uu}^+_x$ ratio is lower in APG than in ZPG.

In order to confirm this influence on scales from a wider range, the energy spectrum using wavelet transformation was calculated. The analysis was done for all measured points throughout the boundary layer thickness for both traverses. The wavelet transformation of each recorded signal was done using a Mexican Hat wavelet function. According to Gordeyev [16], such wavelet function is the best choice to perform analysis of the single events present in the time signal. Iso-contours of the wavelet energy spectra E scaled by the square of friction velocity u_τ as a function of y^+ and the time scale $\tau^+ = \tau u^2_\tau/\nu$ is shown in Figure 3. To remove the effect of convection velocity, the time scale τ was used instead of length scale λ, which was proposed by Marusic *et al.* [17]. The black cross (+) corresponds to the scale and location of near-wall peak of velocity fluctuations, while the upward-triangle (see Figures 5 and 6) corresponds to the scale and location of the outer peak.

Figure 3 shows the comparison of energy spectra for a single-wire probe with wire length $l^+ \approx 16$ and X-wire probe with wire length $l^+ \approx 50$ taken at Sg = 0.185. Figure 3a presents the comparison of streamwise components, while Figure 3b shows the comparison of streamwise for a single-wire probe and wall-normal for X-wire probe components. Dashed lines on both graphs refer to the component measured by a single-wire probe, which is treated as a reference case. The continuous iso-lines for u_x and u_y obtained from X-wire probe are superimposed for comparison. As the energy iso-lines are drawn to the same scales, the lower values of u_x measured by X-wire probe are easily visible

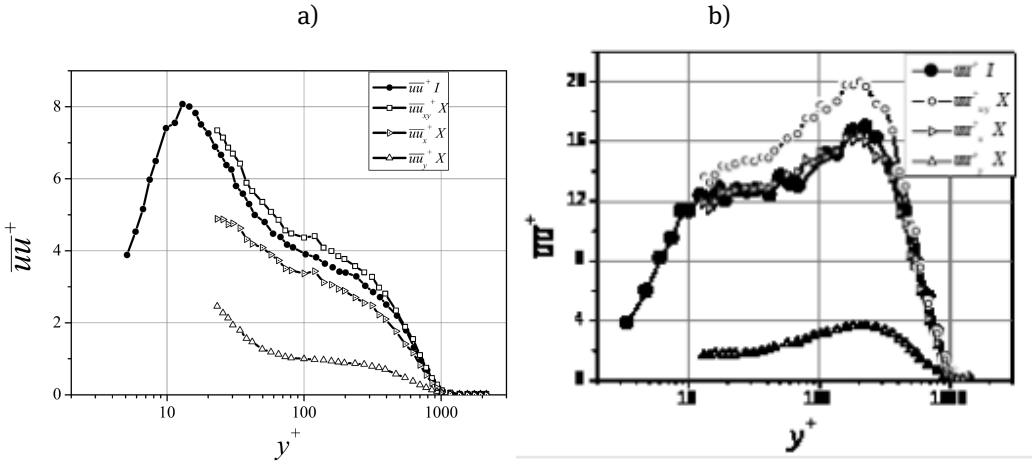

Figure 2: Comparison of fluctuating components from single (I) and X-wire (X) probes; a) for traverse Sg=0.185; b) for traverse Sg=0.738.

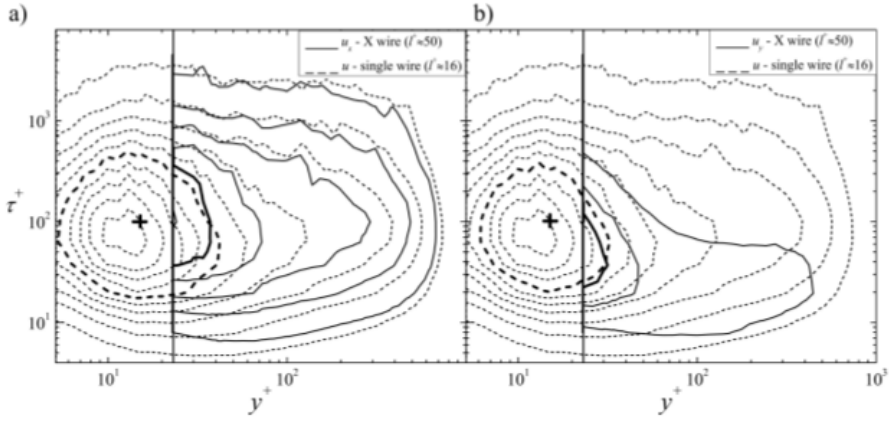

Figure 3: Iso-contours of the energy spectra $\frac{E}{u_\tau^2}$ in ZPG: a) effect of the length scale and geometry of the probe: single-wire $l^+ \approx 16$ (solid); X-wire $l^+ \approx 50$ (dashed) on streamwise energy, and b) comparison of streamwise single-wire and wall-normal X-wire energy. Contours are from 0 to 2 with the steps equal to 0.2.

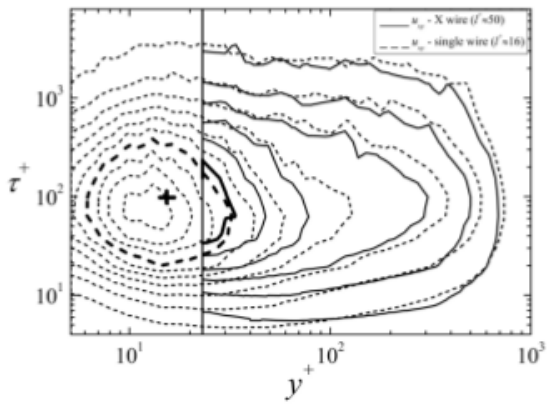

Figure 4: Iso-contours of the energy spectra $E_{u_{xy}} = \left(E_{u_x}^2 + E_{u_y}^2\right)^{\frac{1}{2}}$ component across boundary layer thickness - effect of the probe: X-wire $l^+ = 50$ (solid); single-wire $l^+ = 16$ (dashed). Contours are from 0 to 2 with the steps equal to 0.2.

(see Figure 3a). More interestingly, however, is the maximum shift of X-wire streamwise energy to the higher time scales. For better interpretation, the iso-contours near the maximum of $\frac{E}{u_\tau^2}$ have been drawn by thick lines. This phenomena is observed mainly for small scale ranges below $\tau^+ \approx 100$. Similar effects for a single-wire probe with different lengths of the wire were also observed by Hutchins *et al.* [2]. On the other hand, (Figure 3b) the location of the maximum of u_y energy (solid thick line) is shifted towards smaller scales, the position of which can be estimated near $\tau^+ \approx 60$. Displacement of the u_y maximum in relation to u_x maximum is consistent with the study of Marusic *et al.* [17] and can be explained based on attached eddies hypothesis, according to which the wall-normal fluctuations will lack a large-scale component at the wall due to the blocking effect [18]. It is clear, therefore, that the energy maximum of u_y is shifted towards the smaller scales in comparison to streamwise component, and consequently it must have an impact on readings of a single-wire probe. It is worth noting that the increased wall-normal component appears for the same time scale as the bursting process [19] and should result in overestimation of the near-wall peak captured by a single-wire probe.

In order to demonstrate that the u_y component influences a single-wire probe reading, the resultant fluctuation energy $E_{u_{xy}} = \left(E_{u_x}^2 + E_{u_y}^2\right)^{\frac{1}{2}}$ was compared to single-wire probe fluctuation energy, as shown in Figure 4. It is seen now that $E_{u_{xy}}$ has the maximum (solid thick line) for the scale, which corresponds better to $E_{u_{xy}}$ iso-contours (dashed thick line) obtained for single-wire probe with respect to the results shown in Figure 3a. The scale energy redistribution confirms that the near-wall peak of fluctuation comes from increase of the small-scale component of u_y near the wall.

A similar analysis was conducted for adverse gradient region (Sg = 0.783) and the results are presented in Figure 5. For this type of plot the first peak (+), corresponding to the small-scale component, is clearly visible and its intensity is of similar amplitude indicating that small scales remain almost unaffected by pressure gradient. But the most important difference is the substantial rise of energy observed for a time scale $\tau^+ > 100$. The outer peak can be noticed at location $y^+ = 200$ and $\tau^+ = 120$. The difference between iso-contours of the energy spectra is not so obvious as in the former case, however a slight shift of X-wire streamwise energy to the higher time scales is also noticed close to near-wall peak. The location of the maximum of u_y energy (solid thick line) is shifted towards smaller scales in comparison to streamwise component (Figure 5b), the position of which is near $\tau^+ \approx 20$ and is the same as for zero pressure gradient flow. However, the maximum occurs for $y^+ = 200$. Hence, because of smaller scale of u_y , it is obvious that it must cause a shift in location of energy maximum of single-wire probe. Figure 6 shows the resultant fluctuation energy $E_{u_{xy}} = \left(E_{u_x}^2 + E_{u_y}^2\right)^{\frac{1}{2}}$ compared to single-wire probe fluctuation energy. The shift of maximum onto the smaller scale is not very clear, but it is due to the fact that streamwise fluctuations dominate in the flow for this case. The strong shift is observed for $\tau^+ < 30$ and above the wall distance $(y^+ = 30)$ where the best correction was obtained.

These results show that the single-wire measurements yield not u_x fluctuation, but rather the resultant of u_x and u_y velocity components. Furthermore, this indicates that the near-wall peak of fluctuation obtained by single-wire probe could be overestimated due to the influence of wall-normal component. The influence of wall-normal component occurs not only in the near-wall peak for small-scale structures but also in the APG outer region, where large-scale motion dominates. Another important conclusion of this study is that the criteria for wire length, i.e. $l^+ < 20$, canot be sufficient to properly estimate the streamwise and wall normal fluctuations.

4 Conclusions

This paper discusses the issue of measuring velocity fluctuations of turbulent boundary layer using hot-wire probes. The results showed that the observed difference between streamwise fluctuating component measured with single- and X-wire probes results not only from

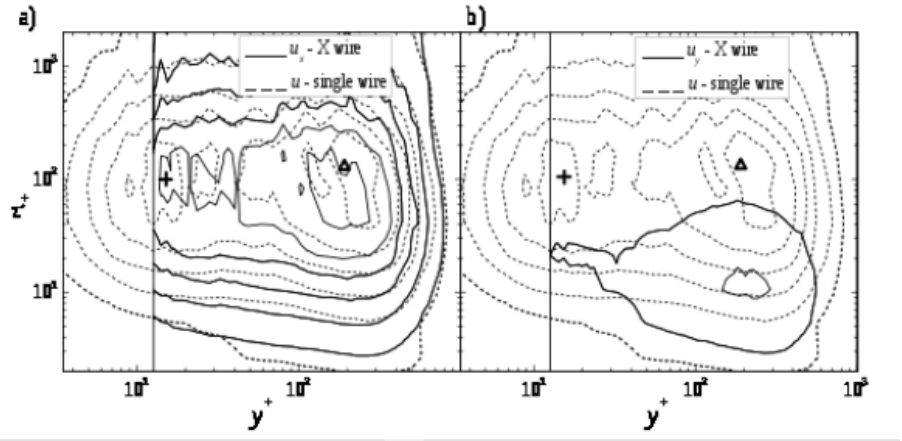

Figure 5: Iso-contours of the energy spectra u_τ^2 in APG: a) effect of the length scale and geometry of the probe: single-wire $l^+ \approx 25$ (solid); X-wire $l^+ \approx 25$ (dashed) on streamwise energy, and b) comparison of streamwise single-wire and wall-normal X-wire energy. Contours are from 0 to 1.2 with the steps equal to 0.2.

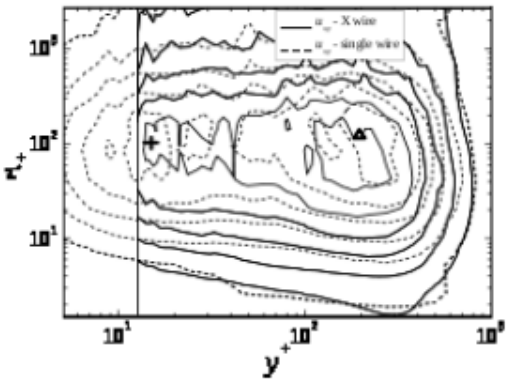

Figure 6: Iso-contours of the energy spectra $E_{u_{xy}} = \left(E_{u_x}^2 + E_{u_y}^2\right)^{\frac{1}{2}}$ component across boundary layer thickness in the APG - effect of the probe: X-wire $l^+ = 25$ (solid); single-wire $l^+ = 25$ (dashed). Contours are from 0 to 1.2 with the steps equal to 0.2.

spatial resolution, but also from influence of wall-normal fluctuating component, which is usually not considered. As a result, the distribution of $\overline{uu}^+$ obtained by means of single-wire probe is slightly overestimated, especially in the wall vicinity. To prove this, the resultant velocity fluctuations from two components obtained from X-wire probe were determined. It has been shown that the resultant velocity fluctuations distribution has the shape of the distribution obtained from a single-wire probe.

In order to confirm this influence on scales from a wider range, the energy spectrum using wavelet transformation was calculated. It was shown that the near-wall peak of single-wire fluctuations is the result of both streamwise and wall-normal small-scale components of velocity fluctuations. It implicates that the underestimation of the near wall-peak of streamwise fluctuating component in Xwire measurements results from the not considered small-scale wall-normal component, which is inherently included in the case of a single-wire probe. For APG case, in spite of lack of spatial averaging effect, the influence of u_y component on single-wire measurements is still present. It was shown that the influence of wall-normal component occurs not only in the near-wall peak for smallscale structures but also in the APG outer region, where large-scale motion dominates.

Acknowledgement: The investigation was supported by National Science Centre under Grant No. DEC2012/07/B/ST8/03791.

References

[1] Ligrani P.M., Bradshaw P., Spatial resolution and measurement of turbulence in the viscous sublayer using subminiature hot-wire probes. Exp. Fluids, 1987, 5, 407–417.

[2] Hutchins N., Nickels T.B., Marusic I., Chong M.S., Hot-wire spatial resolution issues in wall-bounded turbulence. J. Fluid Mech., 2009, 635, 103.

[3] Monty J.P., Chong M.S., Turbulent channel flow: comparison of streamwise velocity data from experiments and direct numerical simulation. J. Fluid Mech., 2009, 633, 461.

[4] Schlatter P., Örlü R., Li Q., Brethouwer G., Fransson J.H.M., Johansson A.V., Alfredsson P.H., Henningson D.S., Turbulent boundary layers up to Re[sub θ]=2500 studied through simulation and experiment. Phys. Fluids, 2009, 21(5), 051702.

[5] Lenaers P., Li Q., Brethouwer G., Schlatter P., Örlü R., Rare backflow and extreme wall-normal velocity fluctuations in near-wall turbulence. Phys. Fluids, 2012, 24(3), 035110.

[6] Dródż A., Elsner W., Comparison of single and X-wire measurements of streamwise velocity fluctuations in turbulent boundary layer. J. Theor. Appl. Mech., 2014, 52(2), 499–505.
[7] Harun Z., Monty J.P., Mathis R., Marusic I., Pressure gradient effects on the large-scale structure of turbulent boundary layers. J. Fluid Mech., 2013, 715, 477–498.
[8] Dróżdż A., Elsner W., Drobniak S., Application of oil-fringe interferometry for measurements of wall shear stress. Turbomachinery, 2008, 133, 103–110.
[9] Dróżdż A., Elsner W., Drobniak S., Scaling of streamwise Reynolds stress for turbulent boundary layers with pressure gradient. Eur. J. Mech. B/Fluids, 2015, 49, 137–145.
[10] Jorgensen F.E., How to measure turbulence with hot-wire anemometers - a practical guide. Dantec Dynamics, Skovlunde, Denmark, 2002.
[11] Örlü R., Alfredsson P.H., On spatial resolution issues related to time-averaged quantities using hot-wire anemometry. Epx. Fluids, 2010, 49(1), 101–110.
[12] Johansson A.V., Alfredsson P.H., Effects of imperfect spatial resolution on measurements of wall-bounded turbulent shear flows. J. Fluid Mech., 1983, 137, 409–421.
[13] Monty J.P., Harun Z., Marusic I., A parametric study of adverse pressure gradient turbulent boundary layers. Int. J. Heat Fluid Flow, 2011, 32(3), 575–585.
[14] Lee J., Sung H.J., Effects of an adverse pressure gradient on a turbulent boundary layer. Int. J. Heat Fluid Flow, 2008, 29(3), 568–578.
[15] Nagano Y., Tsuji T., Houra T., Structure of turbulent boundary layer subjected to adverse pressure gradient. Int. J. Heat Fluid Flow, 1998, 19(5), 563–572.
[16] Gordeyev S., POD, LSE and Wavelet decomposition: Literature Review, University of Notre Dame, Notre Dame, 2000.
[17] Marusic I., Mathis R., Hutchins N., High Reynolds number effects in wall turbulence. Int. J. Heat Fluid Flow, 2010, 31(3), 418–428.
[18] Townsend A.A., The properties of equilibrium boundary layers. J. Fluid Mech., 1956, 1(06), 561.
[19] Dróżdż A., Elsner W., Detection of coherent structures in a turbulent boundary layer with zero, favourable and adverse pressure gradients. J. Phys. Conf. Ser., 2011, 318(6), 062007.